Muon Colliders: New Prospects for Precision Physics and the High Energy Frontier

Bruce J. King[1]

Brookhaven National Laboratory
email: bking@bnl.gov
web page: http://pubweb.bnl.gov/people/bking/

arXiv:hep-ex/9908041v1 8 Aug 1999

Abstract. An overview is given of muon collider technology and of the current status of the muon collider research program. The exciting potential of muon colliders for both neutrino physics and collider physics studies is then described and illustrated using self-consistent collider parameter sets at 0.1 TeV to 100 TeV center-of-mass energies.

INTRODUCTION

Muon colliders appear to be emerging as a promising complement and/or alternative to proton and electron colliders for experimental high energy physics (HEP) studies at the high energy frontier. They also provide some interesting possibilities for precision studies in HEP, particularly in neutrino physics.

This paper consists of three main sections. The first section gives a very brief description of muon collider technology then two longer sections give introductions to the neutrino physics potential and collider physics potential of muon colliders, respectively.

The two physics sections use, as examples, the muon collider parameter sets of table 1, at center of mass (CoM) energies from 0.1 TeV to 100 TeV. The parameter set at 0.1 TeV CoM energy, which is intended as an s-channel Higgs factory, was constrained to essentially reproduce one of the parameter sets currently under study [1] by the Muon Collider Collaboration (MCC). In contrast, the other sets represent speculation by the author on how the parameters might evolve with CoM energy. A discussion and assessment of the technical challenges associated with these specific parameter sets is given in [2]. It should be stressed that they are all still rather speculative (additional to the rather immature status of the entire

[1)] Presented at the Latin American Symposium on High Energy Physics, April 8-11, 1998, San Juan, Puerto Rico. This work was performed under the auspices of the U.S. Department of Energy under contract no. DE-AC02-98CH10886.

TABLE 1. Self-consistent parameter sets for muon colliders at CoM energies ranging from 0.1 TeV to 100 TeV. For completeness, beam parameters and collider ring parameters have been included along with the physics parameters, and the generation and optimization of these parameter sets is described in reference [2]. Except for the first parameter set, which has been studied in some detail by the Muon Collider Collaboration, these parameters represent speculation by the author on how muon colliders might evolve with energy.

center of mass energy, E_{CoM} **description**	0.1 TeV Higgs factory	1 TeV LHC complement	4 TeV E frontier	10 TeV 2^{nd} gen.	100 TeV ult. E scale
collider physics parameters:					
luminosity, $\mathcal{L}$ [$cm^{-2}.s^{-1}$]	1.0×10^{31}	1.0×10^{34}	6.2×10^{33}	1.0×10^{36}	4.0×10^{36}
$\int \mathcal{L}dt$ [fb^{-1}/det/year]	0.1	100	62	10 000	40 000
No. of $\mu\mu \rightarrow$ ee events/det/year	870	8700	340	8700	350
No. of 100 GeV SM Higgs/det/year	3700	69 000	69 000	1.4×10^{7}	8.3×10^{7}
fract. CoM energy spread, σ_E/E [10^{-3}]	0.02	1.6	1.6	1.0	1.0
neutrino physics parameters:					
fract. str. sect. length, f_{ss}	0.15	0.10	0.05	0.04	0.02
neutrino ang. divergence, $\theta_\nu[1/\gamma]$	1	10	10	10	10
high rate det: events/yr/($g.cm^{-2}$)	8.1×10^{6}	1.9×10^{7}	1.5×10^{6}	1.3×10^{8}	2.5×10^{7}
long baseline: events/yr/($kg.km^{-2}$)	1.8×10^{5}	4.2×10^{5}	5.3×10^{5}	2.9×10^{8}	5.6×10^{9}
collider ring parameters:					
circumference, C [km]	0.3	2.0	7.0	15	100
ave. bending B field [T]	3.5	5.2	6.0	7.0	10.5
beam parameters:					
(μ^- or) μ^+/bunch,$N_0[10^{12}]$	4.0	3.5	3.1	2.4	0.18
(μ^- or) μ^+ bunch rep. rate, f_b [Hz]	15	15	0.67	15	60
6-dim. norm. emittance, $\epsilon_{6N}[10^{-12}m^3]$	170	170	170	50	2
x,y emit. (unnorm.) [$\pi.\mu$m.mrad]	710	12	3.0	0.55	0.0041
x,y normalized emit. [π.mm.mrad]	340	57	57	26	1.9
fract. mom. spread, δ [10^{-3}]	0.03	2.3	2.3	1.4	1.4
relativistic γ factor, E_μ/m_μ	473	4732	18 929	47 322	473 220
ave. current [mA]	20	10	0.46	24	4.2
beam power [MW]	1.0	8.4	1.3	58	170
decay power into magnet liner [kW/m]	1.1	0.58	0.03	1.4	1.3
time to beam dump, $t_D[\gamma\tau_\mu]$	no dump	0.5	0.5	no dump	0.5
effective turns/bunch	519	493	563	1039	985
interaction point parameters:					
spot size, $\sigma_x = \sigma_y[\mu m]$	270	7.6	1.9	0.78	0.057
bunch length, σ_z [mm]	11	4.7	1.2	1.1	0.79
β^* [mm]	11	4.7	1.2	1.1	0.79
ang. divergence, σ_θ [mrad]	2.6	1.6	1.6	0.71	0.072
beam-beam tune disruption parameter, $\Delta\nu$	0.013	0.066	0.059	0.100	0.100
pinch enhancement factor, H_B	1.000	1.040	1.025	1.108	1.134
beamstrahlung fract. E loss/collision	5×10^{-16}	1.2×10^{-10}	2.3×10^{-8}	2.3×10^{-7}	3.2×10^{-6}
final focus lattice parameters:					
max. poletip field of quads., $B_{4\sigma}$ [T]	6	10	10	15	20
max. full aperture of quad., $A_{\pm 4\sigma}$[cm]	14	13	30	20	13
β_{max}[km]	0.4	22	450	1100	61 000
final focus demagnification, $\sqrt{\beta_{max}/\beta^*}$	60	2200	19 000	31 000	280 000
synchrotron radiation parameters:					
syn. E loss/turn [MeV]	0.0008	0.01	0.9	17	25 000
syn. rad. power [kW]	0.0002	0.13	0.4	400	110 000
syn. critical E [keV]	0.0006	0.09	1.6	12	1700
neutrino radiation parameters:					
collider reference depth, D[m]	10	125	300	300	300
ave. rad. dose in plane [mSv/yr]	3×10^{-5}	9×10^{-4}	9×10^{-4}	0.66	6.7
str. sect. length for 10x ave. rad., L_{x10}[m]	1.9	1.3	1.1	1.0	2.4
ν beam distance to surface [km]	11	40	62	62	62
ν beam radius at surface [m]	24	8.4	3.3	1.3	0.13

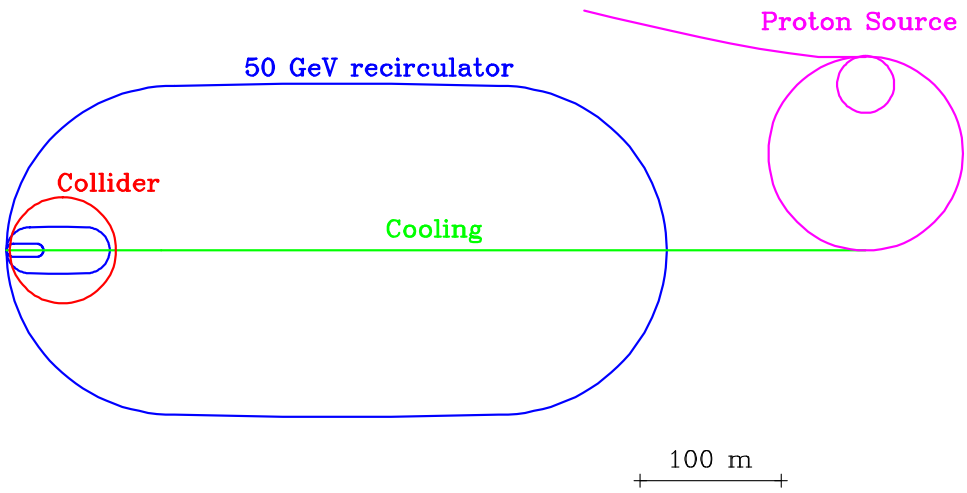

FIGURE 1. Schematic footprint of a 100 GeV muon collider (reproduced from reference [1]).

muon collider technology) and have not been studied or discussed in detail within the MCC. This applies even more strongly to the final parameter set, at 100 TeV, which might represent the ultimate energy scale for muon colliders and which assumes technological extrapolations (in magnets, etc.) that might not come to pass for at least another couple of decades.

AN OVERVIEW OF MUON COLLIDERS

The technology of muon colliders is relatively new. The possibility of muon colliders was introduced by Budker [3], Skrinsky et al. [4] and Neuffer [5] and has been aggressively developed over the past four years in a series of collaboration meetings and workshops [6–9]. A detailed feasibility study for a 4 TeV muon collider [10] was presented at Snowmass96 and, since then, progress has continued on studies for both this collider and others at lower energies. The current status of MCC studies is summarized in [1]. The Muon Collider Collaboration now consists of over 100 physicists and engineers from the U.S.A., Europe and Japan, largely based in the U.S.A. and mainly at three U.S. national laboratories: Brookhaven National Laboratory (BNL), Fermi National Accelerator Laboratory (FNAL) and Lawrence Berkeley National Laboratory (LBNL).

Figure 1 illustrates the basic layout of a $\mu^+\mu^-$collider using, as an example, the schematic footprint of a 0.1 TeV collider. Initially, large bunches of low energy muons are produced by targeting proton bunches from a high intensity proton source onto a pion production target inside a solenoidal capture and decay channel. The relatively diffuse muon bunches from the decay channel then enter an ionization cooling channel, which shrinks them down to a suitable emittance for fast acceleration and injection, at full energy, into a collider storage ring. (The final acceleration stage is anomalously larger than the collider ring for the low energy collider of figure 1. Depending on design and technology choices, the final accelera-

tion stage may well remain larger than the collider ring for higher energy colliders, but likely by a lesser margin.)

The ionization cooling channel is the most novel and characteristic feature of a muon collider, and also the biggest technical challenge. As a general outline of the cooling process, the muons in each bunch lose both transverse and longitudinal momentum in passing through a material medium and are then reaccelerated in radiofrequency (rf) cavities, restoring the longitudinal momentum but leaving a reduced transverse momentum spread in the bunch. Also, the momentum spread of the bunch can be reduced by using wedges of material in a dispersive section of a magnet lattice to reduce preferentially the momenta of the munos with higher momenta. A large amount of cooling is required – current scenarios give a factor of 10^6 reduction in the invariant 6-dimensional phase space – so the cooling channel will probably be a repetitive structure with perhaps 20 to 30 stages. The MCC is pursuing a vigorous theoretical and experimental program to develop and test the components of the cooling channel.

Because of the short muon lifetime – 2.2 microseconds in the muon rest frame – the muon cooling and acceleration must be done very quickly. Current scenarios envisage about a 50% decay loss in the cooling channel and a 25% loss of the remaining muons during acceleration. Also, the muons survive for only of order 1000 turns in the collider ring (almost independent of the collider energy), so the muon bunches must be frequently replenished. Undesirable consequences of the large bunches of muons decaying to electrons are the resulting large and difficult background in the collider detectors, the radiation heat load on the collider ring and, surprisingly, the potential radiation hazard from the intense neutrino beams. The neutrino radiation hazard becomes an important design constraint for high energy colliders, and is discussed in more detail in a later section.

PROSPECTS FOR NEUTRINO PHYSICS

This section gives an overview of the neutrino physics possibilities at a future muon storage ring, which can be either a muon collider ring or a ring dedicated to neutrino physics that uses muon collider technology to store large muon currents. It summarizes a previous more detailed description of these topics by this author [11] (using a generalized description of neutrino production and event rates that is now applicable to all muon colliders).

The section begins with a characterization of the neutrino beam and predictions for neutrino event rates in both general purpose and long-baseline neutrino detectors, then follows with a description of a specific design for a general baseline detector. Finally, an overview is given of some of the important physics analyses that could be performed at such "muon ring neutrino experiments" (MURINE's).

Neutrino Beam and Experimental Overview

Neutrinos are emitted from the decay of muons in the collider ring:

$$\begin{aligned} \mu^- &\rightarrow \nu_\mu + \overline{\nu_\mathrm{e}} + \mathrm{e}^-, \\ \mu^+ &\rightarrow \overline{\nu_\mu} + \nu_\mathrm{e} + \mathrm{e}^+. \end{aligned} \tag{1}$$

The thin pencil beams of neutrinos for experiments will be produced from long straight sections in either the collider ring or a ring dedicated to neutrino physics. From relativistic kinematics, the forward hemisphere in the muon rest frame will be boosted, in the lab frame, into a narrow cone with a characteristic opening half-angle, θ_ν, given in obvious notation by

$$\theta_\nu \simeq \sin\theta_\nu = 1/\gamma = \frac{m_\mu}{E_\mu} \simeq \frac{10^{-4}}{E_\mu(\mathrm{TeV})}. \tag{2}$$

The final focus regions around collider experiments are important exceptions to equation 2 since the muon beam itself will have an angular divergence in these regions that is large enough to spread out the neutrino beam by at least an order of magnitude in both x and y. It is likely that neutrino experiments at sub-TeV CoM energy muon colliders will use the beams from either dedicated or utility straight sections opposite the collider detector while those at higher energy muon colliders – where neutrino radiation is an important design constraint – will use the more divergent beam emanating from the final focus region. A dedicated storage ring could avoid the problem of neutrino radiation by using a long downward-tilting long straight section.

The dominant interaction of TeV-scale neutrinos is deep inelastic scattering (DIS) off nucleons with the production of several hadrons. This is reinterpreted in the quark-parton model as elastic or quasi-elastic scattering off the quark constituents of the nucleons followed by hadronization of the final state quark. Charged current (CC) DIS scattering, which is mediated by a charged W boson and comprises about 75% of the total cross-section, may be represented as

$$\begin{aligned} \nu + q &\rightarrow l^- + q', \\ \overline{\nu} + q' &\rightarrow l^+ + q, \end{aligned} \tag{3}$$

where l is an electron/muon for electron/muon neutrinos and the quarks, (q) and (q'), have charges differing by one unit. Neutral current (NC) DIS scattering,

$$\nu + q \rightarrow \nu + q, \tag{4}$$

which is interpreted as neutrino-quark elastic scattering with the exchange of a neutral Z boson, makes up the remaining 25% of the cross-section.

For TeV-scale neutrinos, the neutrino cross-section is approximately proportional to the neutrino energy, E_ν, and the charged current (CC) and neutral current (NC)

interaction cross sections for neutrinos and antineutrinos have numerical values of [12]:

$$\sigma_{\nu \mathrm{N}} \text{ for } \begin{pmatrix} \nu - CC \\ \nu - NC \\ \overline{\nu} - CC \\ \overline{\nu} - NC \end{pmatrix} \simeq \begin{pmatrix} 0.72 \\ 0.23 \\ 0.38 \\ 0.13 \end{pmatrix} \times \mathrm{E}_{\nu}[\mathrm{TeV}] \times 10^{-35}\ \mathrm{cm}^2. \quad (5)$$

Using these cross-section values, it is straightforward to derive predictions for the approximate neutrino event rates at a neutrino detector. For a general purpose detector subtending the boosted forward hemisphere of the neutrino beam:

$$\text{Number of } \nu \text{ events/yr} \simeq 1.8 \times 10^7 \times l[\mathrm{g.cm}^{-2}] \times \mathrm{f_b}[\mathrm{Hz}] \times \mathrm{N}_0[10^{12}] \times \mathrm{E}_{\mu}[\mathrm{TeV}] \times \mathrm{f_{ss}} \times (1 - \mathrm{e}^{-\mathrm{t_D}[\gamma\tau_{\mu}]}), \quad (6)$$

with notation as in table 1, where l is the detector length, 10^7 seconds of running time per year are assumed and the fractional breakdown into interaction types is as in equation 5.

The analagous equation for a long baseline detector in the center of the neutrino beam is:

$$\text{Number of } \nu \text{ events/yr} \simeq 9 \times 10^6 \times \frac{\mathrm{M[kg]}}{(\mathrm{L[km]})^2 \times (\gamma\theta_{\nu})^2} \times \mathrm{f_b}[\mathrm{Hz}] \times \mathrm{N}_0[10^{12}] \times \mathrm{E}_{\mu}[\mathrm{TeV}] \times \mathrm{f_{ss}} \times (1 - \mathrm{e}^{-\mathrm{t_D}[\gamma\tau_{\mu}]}), \quad (7)$$

where M is the detector mass, L the distance from the neutrino source and the factor $(\gamma\theta_{\nu})^{-2}$ allows for the possibility that the divergence, θ_{ν}, of the neutrino beam is larger than $1/\gamma$. Using these equations, table 1 gives numerical predictions of event rates for each of the parameter sets. Clearly, these can be several orders of magnitude higher than at today's neutrino beams, even when using less massive targets.

A General Purpose Neutrino Detector

Figure 2 is an example of the sort of high rate general purpose neutrino detector that would be well matched to the intense neutrino beams at muon colliders. The neutrino target is a 1 meter long stack of CCD tracking planes with a radius of 10 cm chosen to match the beam radius at approximately 200 meters from production for a 250 GeV muon beam. It contains 750 planes of 300 micron thick silicon CCD's, corresponding to a mass per unit area of approximately 50 $\mathrm{g.cm}^{-2}$, about 2.5 radiation lengths and 0.5 interaction lengths. (Note the contrast with the kilotonne-scale calorimetric targets used in today's high rate neutrino experiments.) For this target, it is seen that the parameter sets in table 1 typically correspond to several hundred million neutrino interactions per year, and the rate could be even higher for a dedicated muon storage ring or more massive target.

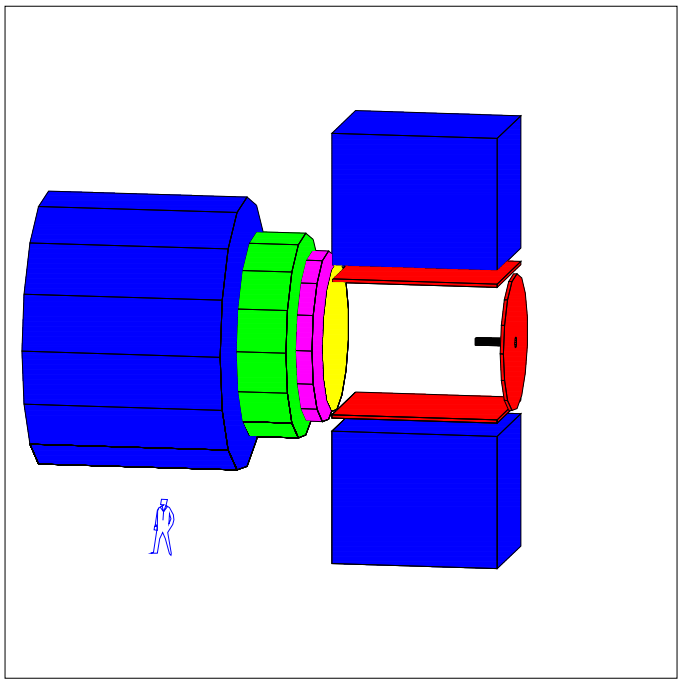

FIGURE 2. Example of a general purpose neutrino detector, reproduced from reference [12]. A human figure in the lower left corner illustrates its size. The neutrino target is the small horizontal cylinder at mid-height on the right hand side of the detector. Its radial extent corresponds roughly to the radial spread of the neutrino pencil beam, which is incident from the right hand side. Further details are given in the text.

Besides providing the mass for neutrino interactions, the tracking target allows precise reconstruction of the event topologies from charged tracks, including event-by-event vertex tagging of those events containing charm or beauty hadrons or tau leptons. Given the favorable vertexing geometry and the few-micron typical CCD hit resolutions, it is reasonable to expect almost 100 percent efficiency for b tagging, perhaps 70 to 90 percent efficiency for charm tagging and excellent discrimination between b and c decays.

The target in figure 2 is surrounded by a time projection chamber (TPC) tracker in a vertical dipole magnetic field. The characteristic dE/dx signatures from the tracks would identify each charged particle. Further particle ID is provided by the Cherenkov photons that are produced in the TPC gas then reflected by a spherical mirror at the downstream end of the tracker and focused onto a read-out plane at the upstream end of the target. The mirror is backed by electromagnetic and hadronic calorimeters and, lastly, by iron-core toroidal magnets for muon ID.

The relativistically invariant quantities that are routinely extracted in DIS experiments are 1) Feynman x, the fraction of the nucleon momentum carried by the struck quark, 2) the inelasticity, $y = E_{\mathrm{hadronic}}/E_{\nu}$, which is related to the scattering angle of the neutrino in the neutrino-quark CoM frame, and 3) the momentum-transfer-squared, $Q^2 = 2M_{\mathrm{proton}}E_{\nu}xy$. As a significant advance, this detector will

have the further capability of accurately reconstructing the hadronic 4-vector, resulting in a much better characterization of each interaction, particularly for NC interactions.

Another big improvement over today's neutrino detectors is the vastly improved ability to reconstruct the flavor of the final state quark. Final state c and b quarks can be identified by vertex tagging of the decaying charm or beauty hadrons that contain them, and some statistically based flavor tagging will also be available for u, d or s final state quarks, taking advantage of the "leading particle effect" that is used, for example, in LEP analyses of hadronic Z decays.

Neutrino Physics Opportunities

Neutrino interactions are interesting both in their own right and as probes of the quark content of nucleons, so a MURINE has wide-ranging potential to make advances in many areas of elementary particle physics. This section gives an overview for measurements involving the Cabbibo-Kobayashi-Maskawa (CKM) quark mixing matrix, nucleon structure and QCD, electroweak measurements, neutrino oscillations and, finally, studies of charmed hadrons.

With huge samples of flavor tagged events, a MURINE should be able to make impressive measurements of the absolute squares of several of the elements in the CKM quark mixing matrix. The analyses would be analagous to, but vastly superior to, current neutrino measurements of $|V_{cd}|^2$ that use dimuon events for final state tagging of charm quarks. The current, experimentally determined values for the 9 mixing probabilities are given in table 2 [13], along with their current percentage uncertainties and speculative projections [11] for how 4 of the 9 uncertainties could be reduced by a MURINE at a 500 GeV CoM muon collider. Additionally, if muon colliders eventually reach the 100 TeV energy scale then the associated neutrino beams will even produce final states containing a top quark, almost certainly resulting in uniquely precise determinations of $|V_{td}|^2$ and $|V_{ts}|^2$.

Another major motivation for MURINE's is the potential for greatly improved measurements of nucleon structure functions (SF). Knowledge of these SF's is crucial for precision measurements in neutrino physics, charged lepton scattering experiments and some precision analyses at proton-proton and lepton-proton colliders. Further, they provide important tests of quantum chromodynamics (QCD), and a MURINE might well be the best single experiment of any sort for the examination of perturbative QCD [11].

Neutrino physics has also had an important historical role in measuring the electroweak mixing angle, which is simply related to the mass ratio of the W and Z intermediate vector bosons:

$$\sin^2\theta_W \equiv 1 - \left(\frac{M_W}{M_Z}\right)^2. \tag{8}$$

(To be precise, this is the Sirlin on-shell definition of $\sin^2\theta_W$.)

TABLE 2. Absolute squares of the elements in the Cabbibo-Kobayashi-Maskawa (CKM) quark mixing matrix. The second row for each quark gives current percentage uncertainties in quark mixing probabilities and speculative projections of the uncertainties after analyses on 10^{10} events from a MURINE at a 500 GeV CoM muon collider. The two uncertainties in brackets have not been measured directly from tree level processes. The uncertainties assume that no unitarity constraints have been used.

	d	**s**	**b**
u	**0.95**	**0.05**	**0.00001**
	$\pm$0.1%	$\pm$1.6%	$\pm$50% $\rightarrow$ 1-2%
c	**0.05**	**0.95**	**0.002**
	$\pm$15% $\rightarrow$ 0.2-0.5%	$\pm$35% $\rightarrow \sim$ 1%	$\pm$15% $\rightarrow$ 3-5%
t	**0.0001**	**0.001**	**1.0**
	($\pm$25%)	($\pm$40%)	$\pm$30%

Now that M_Z has been precisely measured at LEP, measurements of $\sin^2\theta_W$ in neutrino physics can be directly converted to predictions for the W mass. The comparison of this prediction with direct M_W measurements in collider experiments constitutes a precise prediction of the SM and a sensitive test for exotic physics modifications to the SM [14]. Reference [11] estimates that the predicted uncertainty in M_W from a MURINE analysis might be of order 10 MeV, which improves by an order of magnitude on today's neutrino experiments [14,15] and is approximately equal to the projected best direct measurements from future collider experiments.

There are currently several experimental indications [16] that neutrinos might have non-zero masses and oscillate in flight between the flavor eigenstates. The probability for an oscillation between two of the flavors is given by [17]:

$$\text{Oscillation Probability} = \sin^2\theta \times \sin^2\left(1.27\frac{\Delta \mathrm{m}^2[\mathrm{eV}^2].\mathrm{L[km]}}{\mathrm{E}_\nu[\mathrm{GeV}]}\right), \tag{9}$$

where the first term gives the mixing strength and the second term gives the distance dependence. Reference [11] obtains the following order-of-magnitude mass limit for an assumed long-baseline detector with reasonable parameters and with full mixing:

$$\Delta \mathrm{m}^2|_{\min} \sim \mathrm{O}(10^{-4})\ \mathrm{eV}^2, \tag{10}$$

relatively independent of the distance to the detector. Similarly, a mixing probability sensitivity for 10^{10} events in a short-baseline detector is found to be as low as

$$\sin^2\theta|_{\rm min} \sim {\rm O}(10^{-7}), \tag{11}$$

for the most favorable value of Δm^2. Both of these estimates apply generically to all 3 possible mixings between 2 flavors: $\nu_e \leftrightarrow \nu_\mu$, $\nu_e \leftrightarrow \nu_\tau$ and $\nu_\mu \leftrightarrow \nu_\tau$. (See also reference [18] for another discussion of neutrino oscillations at a MURINE.)

The Δm^2 estimate is more than an order of magnitude better than any proposed accelerator or reactor experiments for $\nu_\mu \leftrightarrow \nu_\tau$ and $\nu_e \leftrightarrow \nu_\tau$, and is competitive with the best such proposed experiments for $\nu_e \leftrightarrow \nu_\mu$. The estimated value for $\sin^2\theta|_{min}$ is even more impressive – orders of magnitude better than in any other current or proposed experiment for each of the three possible oscillations. Such an experiment would either convincingly refute or accurately characterize the claimed observations of oscillations by both the LSND and Super-Kamiokande collaborations.

As an interesting final topic, MURINE's should be rather impressive factories for the study of charm – with a clean, well reconstructed sample of several times 10^8 charmed hadrons produced in 10^{10} neutrino interactions. There are several interesting physics motivations for charm studies at a MURINE [19]. As an example, particle-antiparticle mixing has yet to be observed in the charm sector [20], and it is quite plausible [11] that a MURINE would provide the first observation of $\rm D^0 - \overline{D^0}$ mixing.

MUON COLLIDER SCENARIOS

This section explores the collider physics opportunities at muon colliders through reference to the example collider parameter sets of table 1. Complementary discussion on the collider physics aspects of these parameters can be found in [2], where it is opined that each parameter set has some aspects that appear challenging but none of the parameter sets are obviously implausible. Admittedly, table 1 gives a rather incomplete sampling of the possibilities and, for example, discussions of additional physics options with sub-TeV muon colliders may be found in [21].

The section begins with a discussion on muon collider design constraints due to the potential neutrino radiation hazard – a serious problem that is unique to muon colliders – before examining, in turn, the physics potential of each of the parameter sets in table 1.

The Potential Radiation Hazard from Neutrinos

A serious and unexpected problem that has arisen for multi-TeV $\mu^+\mu^-$colliders is the potential radiation hazard posed by neutrinos emitted from muon decays in the collider ring [22,23]. These neutrinos produce a "radiation disk" in the plane of the ring, and the potential radiation hazard results from the showers of ionizing particles from occasional neutrino interactions in the soil and other objects bathed by this disk. Although the neutrino cross-section is tiny, this is greatly compensated

by the enormous number of tightly collimated high energy neutrinos produced at the collider ring.

With some reasonable assumptions, the approximate average numerical value for the annual radiation dose in the plane of the collider ring is easily derived to be [23]:

$$D_{ave}[\mathrm{mSv/yr}] \simeq 0.044 \times \frac{f_b[\mathrm{Hz}] \times N_0[10^{12}] \times (1 - e^{-t_D[\gamma\tau_\mu]}) \times (E_\mu[\mathrm{TeV}])^3}{D[\mathrm{m}]}, \quad (12)$$

with notation as in table 1 and assuming an accelerator running time of 10^7 seconds per year. For comparison, the U.S. federal off-site radiation limit is 1 mSv/year, which is of the same order of magnitude as the typical background radiation from natural causes (i.e. 0.4 to 4 mSv/yr [17]).

To explain the form of equation 12, the inverse dependence of the neutrino radiation on the collider depth arises because the radiation levels fall as the inverse square of the distance from the ring while the distance to reach the Earth's surface, assuming a spherical Earth, goes as the square root of the depth. Also, the cubic dependence on the collider energy comes from combining the approximately linear rises with energy of a) the neutrino cross section b) the energy deposited per interaction, and c) the beam intensity due to the decreasing angular divergence of the neutrinos in the vertical plane(equation 2). (There are actually some mitigating factors that come into play at the highest energies and are not included in equation 12 [23].)

This equation is not intended to be accurate at much better than an order of magnitude level and is deliberately conservative, i.e. it may well overestimate the radiation levels. Because of the energy dependence, the radiation levels rapidly become a serious design constraint for colliders at the TeV scale and above.

The radiation intensity may be greatly enhanced downstream from straight sections in the collider ring, with the additional intensity rising in proportion to the length of the straight section. As a benchmark, the length of straight section to produce ten times the planar average dose, L_{x10}, may be shown [23] to be approximately:

$$L_{x10}[\mathrm{meters}] \simeq 0.3 \times \frac{C[\mathrm{km}]}{E_\mu[\mathrm{TeV}]}. \quad (13)$$

This equation shows that the intensity from the straight section picks up another power of the collider energy, which is due to the falling horizontal angular divergence, but this is approximately compensated for by the collider circumference also rising in approximate proportion to the beam energy. As can be seen from table 1, L_{x10} is only of order a meter at all collider energies, so great care must be taken in the design of the collider ring to minimize or eliminate long straight sections.

Because of the cubic rise with energy of the neutrino radiation intensity, muon colliders at CoM energies of beyond a few TeV will probably have to be constructed at isolated sites where the public would not be exposed to the neutrino radiation disk. Such sites clearly exist, perhaps even with useful existing infrastructure.

(An extreme example would be close to a nuclear test site, such as in Nevada, U.S.A.) These will presumably be "second generation" machines, arriving after the technology of muon colliders has been established in one or more smaller and less expensive machines built at existing HEP laboratories.

An S-Channel Higgs Factory

Besides exploring the physics at the energy frontier, muon colliders with very narrow CoM energy spreads are particularly suited to both resonance production and threshold studies of elementary particles. The principal example of such a resonant process is the s-channel production of Higgs bosons. The relatively strong coupling strength of muons to the Higgs channel – approximately 40 000 times that for electrons – gives $\mu^+\mu^-$colliders a unique potential to study this process.

The first parameter set in table 1 is intended for precision studies of a 100 GeV SM-like Higgs boson, hypothesized to have been discovered previously at either LEP, the Tevatron or the LHC. (Of course, the CoM energy of the collider would actually be fixed at the true Higgs mass.) The low CoM energy spread has been chosen to reproduce the predicted width of a SM Higgs at this energy: 2 to 3 MeV. After an initial coarse scan to find the exact energy of the resonance, a fine scan of the resonance would provide uniquely precise measurements of the Higgs mass, width and cross-section.

The technological issues specific to these Higgs factory parameters have been evaluated in some detail over the past year by the MCC [1]. For example, a collider magnet lattice has been designed for the narrow momentum spread beam and the required precise beam calibration was found to be possible by measuring the rate of the muon spin precession.

The physics case for an s-channel Higgs factory has also been studied in some detail [21]. The effectiveness of the collider obviously depends on the existence of a Higgs boson in the appropriate mass range. If the Higgs is too light then, at currently assumed luminosities, the signal will be buried in the backgrounds from the Z resonance. On the other hand, the Higgs width increases with mass, becoming too broad for effective study beyond about 150 GeV. The following approximate scenarios emerge for a SM or SM-like (e.g. supersymmetric) Higgs:

1. $M_H < 105$ GeV: probable discovery at LEP. Backgrounds probably too high for an s-channel Higgs factory.

2. 105 GeV $< M_H <$ 150 GeV: fairly likely to be discovered at FNAL but with poor mass resolution. An s-channel Higgs factory will become useful following more precise M_H measurements from the LHC and/or a future lepton collider with a CoM energy of a few hundred GeV.

3. $M_H > 150$ GeV (this is now experimentally disfavored): the resonance would be too broad for an s-channel factory.

4. (for completeness) no Higgs. A Higgs factory is obviously not useful.

As an example of a detailed study for the Higgs mass in a favorable region, reference [21] makes predictions for 0.4 fb^{-1} of on-peak data and a SM-like Higgs with $M_H = 110$ GeV. They predict a resolution of approximately 0.1 MeV on the Higgs mass, 0.5 MeV on the width and branching ratio determinations as accurate as 3 percent (for the $H \rightarrow b\overline{b}$ channel). These precise measurements on such an important elementary particle clearly provide strong motivation for this muon collider option, either as a stand-alone "first muon collider" or as a relatively inexpensive add-on to a complex with a higher energy machine.

A 1 TeV Muon Collider to Complement the LHC

The motivation for a 1 TeV muon collider would be roughly the same as that of proposed e^+e^-linear colliders at the 1 TeV energy scale – that is, to perform precision studies on whatever elementary particles are discovered at the LHC hadron collider and to search for new particles that will not be evident in the physical and experimental conditions of the LHC. Thus, a 1 TeV muon collider may be considered as a valuable back-up technology in case electron colliders at this energy either run into unforeseen technical difficulties or are found to be unacceptably expensive. Further, such a muon collider may have a role to play even if a 1 TeV e+e- collider is built, due to potentially different physics processes (e.g. Higgs-type particle production) and also to differences in the beam specifications, as follows.

One TeV electron colliders should be able to achieve higher levels of polarization than their muon collider counterparts, which may have polarization levels in the region of 20% [10]. On the other hand, beamstrahlung at 1 TeV electron colliders will result in roughly a 10% fractional spread in collision energy rather than the parts-per-mil spreads assumed for muon colliders. Thus, electron colliders will be favored for studies where high polarization is important while muon colliders should do better in studies of resonances and in other processes where the CoM energy constraint is important.

The 1 TeV parameter set of table 1 would give about the same luminosity as, for example, the design for the proposed NLC linear electron collider [24] at the same energy, and the physics motivation and capabilities might be relatively similar. Placement of the collider at 125 meters depth (the approximate depth of the existing LEP/LHC tunnel at CERN) reduces the average neutrino radiation in the collider plane to less than one thousandth of the U.S. federal off-site radiation limit. (As already mentioned, attention would still need to be paid to minimizing the length of any low-divergence straight sections in the collider ring.)

A Muon Collider at the Energy Frontier: 4 TeV

Muon colliders appear to have much greater potential than electron colliders to push to lepton collision energies above the LHC mass reach (which might be roughly

1 to 2 TeV, depending on the process). The 4 TeV parameter set was chosen as being at about the highest energy that is practical for a "first generation" muon collider on an existing laboratory site, due to neutrino radiation.

The same comments about neutrino radiation apply as in the 1 TeV design and, in addition, it is necessary to greatly reduce the muon current, accepting the consequent loss in luminosity. The assumed 300 meter depth happens to correspond approximately to appropriate bedrock formations at both the BNL and Fermilab HEP laboratories.

Even the reduced luminosity of this parameter set, $6.2 \times 10^{33}\text{cm}^{-2}.\text{s}^{-1}$, appears sufficient to discover whatever elementary particles lie in the mass range of 1 to 4 TeV (i.e. beyond the reach of the LHC), provided only that the experimental signature for production is not particularly obscure and the production cross-section is not greatly suppressed relative to typical SM couplings (as exemplified by the benchmark process, $\mu\mu \rightarrow \text{ee}$).

An added motivation for building a "first generation" muon collider at the highest possible energy is that this would provide the best technical foundation for construction of the very high energy, high luminosity muon colliders (10 TeV and above) that are the ultimate goal of muon collider technology.

A Second Generation Muon Collider at 10 TeV

The 4th parameter set of table 1 specifies a "second generation" muon collider at 10 TeV CoM energy, assumed to be constructed at a site where neutrino radiation is not a constraint (see the previous subsection on neutrino radiation). It is seen that the relaxed neutrino radiation constraint might allow an exciting luminosity of $1.0 \times 10^{36}\text{cm}^{-2}.\text{s}^{-1}$ at several times the discovery mass reach of the LHC, making this collider an exciting prospect for the future progress of HEP.

Besides mapping out the spectrum of elementary particles in the energy decade up to 10 TeV, it is further reasonable to assume that anything already discovered at the LHC could be more fully studied in the much cleaner physics environment of such a lepton collider. Particles in the 100 GeV to 1 TeV range should be copiously produced through higher order processes in a 10 TeV muon collider, as evidenced by the production, via the WW-fusion process, of order ten million SM Higgs particles per year (assuming it exists with a mass below 1 TeV).

The technical difficulties specific to muon colliders at this energy scale and above have yet to be assessed in detail. It is comforting that relativistic kinematics makes the acceleration of the muons progressively easier at higher energies due to a rising muon lifetime, shrinking transverse bunch size and reduced sensitivity to disruptive influences such as wake fields. On the other hand, detector backgrounds involving high energy muons will clearly become more challenging, as will the design and layout of the final focus magnets around the ip (see [2] for details). To put this in perspective, these technical challenges will need to be compared with the considerable challenges that are essentially independent of the collider energy –

particularly the construction and operation of the muon cooling channel.

The Ultimate Energy Scale for Muon Colliders: 100 TeV

The highest energy parameter set in table 1, at 100 TeV, represents what is likely the ultimate energy scale for muon colliders, with a mass reach for discovering elementary particles that is probably inaccessible even to hadron colliders.

The parameter set assumes technical extrapolations beyond today's limits and presents easily the most difficult design challenge of all the parameter sets, for the following reasons:

- cost reductions will be needed to make a machine of this size affordable
- siting will be more difficult than at 10 TeV, since the neutrino radiation is now well above the U.S. federal limit
- the final focus design is much more difficult even than at 10 TeV, as illustrated by the much larger demagnification factor (see [2] for further discussion)
- the muon bunches, although much smaller than in the other sets, are also much cooler (again, see [2] for further discussion)
- the beam power has risen to 170 MW, with synchrotron radiation rising rapidly to contribute a further 110 MW.

It seems reasonable to assume that the rapid rise to prominence of the synchrotron radiation will effectively prohibit muon colliders at the PeV energy scale, even if the other challenges could be negotiated.

A 100 TeV muon collider is clearly not a near-term prospect. However, the unique opportunity to explore the physics at this energy scale could well turn out to be crucial in unlocking the profound mysteries of the elementary particle spectrum and its role in the universe. With such compelling motivation, it is certainly not ruled out that a muon collider at this energy scale could become achievable after a couple of decades of dedicated research and development.

SUMMARY

An overview has been given of the potential prospects for neutrino physics and collider physics at muon colliders and it has been shown that muon colliders may well come to assume a central role in the future of experimental high energy physics. Their discovery reach for new elementary particles might eventually be in the region of 100 TeV and they could also open up exciting new vistas in neutrino physics and other precision studies.

This provides strong motivation for a continuing and expanding vigorous research and development program in muon collider technology, and such a program will be needed to make muon colliders a reality on an attractive timescale.

REFERENCES

1. The Muon Collider Collaboration, "Status of Muon Collider Research and Development and Future Plans", to be submitted to Phys. Rev. E.
2. B.J. King, *Discussion on Muon Collider Parameters at Center of Mass Energies from 0.1 TeV to 100 TeV*, BNL CAP-223-MUON-98C, submitted to Proc. Sixth European Particle Accelerator Conference (EPAC'98), 22-26 June,1998, Stockholm, Sweden, available at http://pubweb.bnl.gov/people/bking/.
3. G.I. Budker, *Accelerators and Colliding Beams*, talk at 7th Internat. Accelerator Conference, Erevan (1969); talk at the Internat. High Energy Physics Conference, Kiev (1970).
4. E. A. Perevedentsev and A. N. Skrinsky, Proc. 12th Int. Conf. on High Energy Accelerators, F. T. Cole and R. Donaldson, Eds., (1983) 485; A. N. Skrinsky and V.V. Parkhomchuk, Sov. J. of Nucl. Physics **12**, (1981) 3; *Early Concepts for $\mu^+\mu^-$ Colliders and High Energy μ Storage Rings*, *Physics Potential & Development of $\mu^+\mu^-$ Colliders. 2^{nd} Workshop*, Sausalito, CA, Ed. D. Cline, AIP Press, Woodbury, New York, (1995).
5. D. Neuffer, IEEE Trans. **NS-28**, (1981) 2034.
6. *Proceedings of the Mini-Workshop on $\mu^+\mu^-$ Colliders: Particle Physics and Design*, Napa CA, Nucl Inst. and Meth., **A350** (1994) ; Proceedings of the Muon Collider Workshop, February 22, 1993, Los Alamos National Laboratory Report LA- UR-93-866 (1993) and *Physics Potential & Development of $\mu^+\mu^-$ Colliders 2^{nd} Workshop*, Sausalito, CA, Ed. D. Cline, AIP Press, Woodbury, New York, (1995).
7. Transparencies at the *2 + 2 TeV $\mu^+\mu^-$ Collider Collaboration Meeting*, Feb 6-8, 1995, BNL, compiled by Juan C. Gallardo; transparencies at the *2 + 2 TeV $\mu^+\mu^-$ Collider Collaboration Meeting*, July 11-13, 1995, FERMILAB, compiled by Robert Noble; Proceedings of the 9th Advanced ICFA Beam Dynamics Workshop, Ed. J. C. Gallardo, AIP Press, Conference Proceedings 372 (1996).
8. D. V. Neuffer and R. B. Palmer, Proc. European Particle Acc. Conf., London (1994); M. Tigner, in Advanced Accelerator Concepts, Port Jefferson, NY 1992, AIP Conf. Proc. **279**, 1 (1993).
9. R. B. Palmer et al., *Monte Carlo Simulations of Muon Production*, *Physics Potential & Development of $\mu^+\mu^-$ Colliders 2^{nd} Workshop*, Sausalito, CA, Ed. D. Cline, AIP Press, Woodbury, New York, pp. 108 (1995); R. B. Palmer, et al., *Muon Collider Design*, in Proceedings of the Symposium on Physics Potential & Development of $\mu^+\mu^-$ Colliders, Elsevier.
10. *$\mu^+\mu^-$ Collider: A Feasibility Study*, BNL-52503, Fermilab-Conf-96/092, LBNL-38946, July 1996.
11. B.J. King, *Neutrino Physics at a Muon Collider*, Proc. Workshop on Physics at the First Muon Collider and Front End of a Muon Collider, Fermilab, November 6-9, 1997.
12. See, for example, Chris Quigg, *Neutrino Interaction Cross Sections*, FERMILAB-Conf-97/158-T.
13. Values extracted from Andrzej J. Buras, *CKM Matrix: Present and Future*, TUM-HEP-299/97.

14. Janet M. Conrad, Michael H. Shaevitz and Tim Bolton, *Precision Measurements with High Energy Neutrino Beams*, hep-ex/9707015, submitted to Rev. Mod. Phys. (1997)
15. K.S. McFarland *et al.* (CCFR/NuTeV Collaboration) *A Precision Measurement of Electroweak Parameters in Neutrino-Nucleon Scattering*, FNAL-Pub-97/001-E. B.J. King, Columbia University Ph.D. Thesis, 1994; Nevis Report: Nevis-283, CU-390, Nevis Preprint R-1500 (1994).
16. LSND Collaboration, *Evidence for numu to nue Oscillations from Pion Decay in Flight Neutrinos* (Updated June 12,1997), submitted to PRC, LA-UR-97-1998, UCRHEP-E191; Super-Kamiokande Collaboration, *Measurement of a small atmospheric ν_μ/ν_e ratio* (February 12, 1998), submitted to Phys. Lett. B.
17. R.M. Barnett et al., Physical Review D54, 1 (1996) and 1997 off-year partial update for the 1998 edition available on the PDG WWW pages (URL: http://pdg.lbl.gov/).
18. S. Geer, *The Physics Potential of Neutrino Beams From Muon Storage Rings*, Proc. Workshop on Physics at the First Muon Collider and Front End of a Muon Collider, Fermilab, November 6-9, 1997.
19. I.I Bigi, *Open Questions in Charm Decays Deserving an Answer*, CERN-TH.7370/94, UND-HEP-94-BIG08 (1994). I.I Bigi, *The Expected, The Promised and the Conceivable - on CP Violation in Beauty and Charm Decays.*, UND-HEP-94-BIG11 (1994).
20. Tiehui (Ted) Liu, *The D0-Dobar Mixing Search – Current Status and Future Prospects*, HUTP-94/E021 (1994). Gustavo Burdman, *Charm Mixing and CP Violation in the Standard Model*, FERMILAB-Conf-94/200 (1994).
21. Proc. Workshop on Physics at the First Muon Collider and Front End of a Muon Collider, Fermilab, November 6-9, 1997, Ed. S. Geer and R. Raja.
22. B.J. King, *Assessment of the prospects for muon colliders*, paper submitted in partial fulfillment of requirements for Ph.D., Columbia University, New York (1994).
23. B.J. King, *A Characterization of the Neutrino-Induced Radiation Hazard at TeV-Scale Muon Colliders*, BNL Center for Accelerator Physics internal report 162-MUON-97R, to be submitted for publication.
24. The NLC Design Group, *Zeroth-Order Design Report for the Next Linear Collider* (May, 1996), LBNL-5424, SLAC-474, UCRL-ID-124161, UC-414.